



# Experimental study on heat transfer in soil during heat storage and release processes

Feiyu Zhu<sup>1</sup> · Yasu Zhou<sup>1</sup> · Shuiping Zhu<sup>1</sup>

Received: 9 October 2020 / Accepted: 26 February 2021 / Published online: 7 March 2021  
© The Author(s), under exclusive licence to Springer-Verlag GmbH Germany, part of Springer Nature 2021

## Abstract

The soil temperature distribution characteristics were experimentally studied, during heat storage and release processes in the fine-grained sand with different moisture content. Results showed that, the soil temperature distributions in the process of soil heat storage and release are almost symmetric under the same excess temperature. The excess temperature is the main factor affecting the soil temperature change, and the influence of the moisture content variation is almost negligible. At each set of excess temperature, the soil temperature change in heat storage and release processes have a good logarithmic relationship with the heat transfer time, radial distance and longitudinal distance. The soil temperature change shows a linear increase trend with the excess temperature, and the soil temperature disturbance in radial direction is far greater than that in longitudinal direction. Based on the hypothetical multivariate nonlinear power function regression model, the experience formula for predicting the soil temperature was proposed. The prediction deviation was within 10 %.

**Keywords** Fine-grained sand · Excess temperature · Moisture content · Heat storage and release · Soil temperature distribution

## 1 Introduction

Porous media is a kind of composite media composed of multi-phase materials. The solid matrix is usually used as the skeleton. The pores between the solid frameworks are filled with liquid phase, gas phase or gas-liquid mixture phase fluids, and the pores distribution is random and non-directional. The heat migration in porous media is often accompanied by the moisture migration [1], the heat and moisture migration are coupled with each other [2], which follows the basic law of heat and mass conservation, and the capillary flow is the dominant mechanism that governs the moisture transfer [3]. In the non-chemical reaction process, the pressure potential, temperature potential and concentration potential are the main driving forces of heat and mass transfer in porous media. The heat transfer process mainly includes solid heat conduction, convection and phase change heat transfer (which can be ignored, when the particle size of the porous media is less than 4–6 mm, and  $Gr$  (Grachev number)  $\times Pr$  (Prandtl number)  $< 10^3$ ),

and radiation heat transfer (which is obvious, when there is a high temperature difference between solid particles). The mass migration process mainly includes molecular diffusion, capillary diffusion and osmotic diffusion [4].

Soil is a kind of typical anisotropic porous media, which has all the basic physical properties of porous media. The temperature and humidity gradient, solute concentration and water vapor content are the leading driving forces influencing the processes of heat and mass transfer in unsaturated soil [5], and the soil temperature field would strongly influence the soil properties [6]. Some scholars [7–14] had made relevant theoretical studies on the coupled heat and moisture migration characteristics in porous media, results showed the temperature and humidity variation during the coupled heat and moisture migration process and the affect factors on that. In addition to transport phenomena, influence of continuing hydration resulted by rising temperature on the moisture distribution also can't be ignored [15].

Based on the high-temperature thermal storage system in soils, Wang et al. [16–18] experimentally studied the temperature and humidity variation in the fine sand during heat storage processes, and analyzed the influences of the inlet fluid temperature (60 and 80 ) and initial moisture content (0.7 %, 4.6 %, 6.2 %, 9.1 %) on the thermal performance of borehole heat exchanger, results showed that, the soil temperature and humidity near the tube wall may appear a temporary peak

✉ Yasu Zhou  
zhouys@dhu.edu.cn

<sup>1</sup> College of Environmental Science and Engineering, Donghua University, Shanghai 201620, China

value, the peak temperature phenomenon in the soil becomes weakened with the gradually increase of the distance from the tube wall, and the heat transfer rate of the borehole heat exchanger increases with the increase of injection temperature. Hedayati-Dezfooli et al. [19] experimentally studied the one-dimensional heat and moisture transfer in the medium coarse soil with a porosity and an initial moisture content of 0.40 and 0.26, at four different temperature levels within the range of 40 ~ 90 , results showed that the thermal vapor diffusion is the main mechanism for the moisture flux under the above setting conditions. Wang et al. [20] experimentally studied that the temperature of the ramming ground surface in sandy silt with groundwater is 3.5 % higher than that without groundwater under low indoor temperature, and Liu et al. [21] concluded that the dry surface layer in soil has a stronger influence on the heat and moisture transfer. Moradi et al. [22] indicated that the heat injection and extraction efficiency will be significantly affected by thermally induced water flow in the vadose zone, the results showed that the thermally induced water flow and convective heat transfer cannot be neglected when modeling soil-borehole thermal energy storage systems under unsaturated condition, which validated by the laboratory-scale tank tests. Li et al. [23] experimentally compared the heat and moisture transfer of the sand with that of the sand/bentonite mixtures under the heating operation conditions (the temperature for the thermostatic water bath was kept as 40°C) and cooling operation conditions (the temperature for the thermostatic water bath was kept as 7°C). Zhao et al. [24] investigated the thermal characteristics of the saturated soil around coaxial GCHE (ground coupled heat exchanger) through experimental study (based on artificial glass micro-balls as porous medium) and theoretical analysis (based on Darcy's natural convection), the results indicated that heat transfer mainly happens near the outer wall of coaxial GCHE and inclines to stabilization at far-field, and the inlet temperature, initial temperature of porous medium, flow rate are major factors affecting heat transfer. Not only in the GSHP field, studying the coupled heat and moisture migration of porous media has practical application significance in the design of heat dissipation of underground cables [25], porous building materials [26] and so on.

Based on the above analysis, most scholars had conducted the related experimental researches on the characteristics of the soil heat and moisture migration during heat storage process or heat release process, which were under the different temperature and humidity conditions. It is still unable to compare the heat transfer performance of the soil in heat storage and release processes. In this paper, the comparative analysis of the heat transfer during the process of soil heat storage and release under the same temperature and humidity conditions will be conducted. It is also expected to obtain an experience formula for predicting the soil temperature change.

## 2 Experimental setup

In order to study the heat transfer during the process of soil heat storage and release, the specially-designed experimental setup was built. The schematic of the experimental setup was shown in Fig. 1, wherein the heat exchange unit and the circulation loop were all wrapped with insulation cotton (thickness of 15mm) and reflective aluminum foil to further weaken the heat loss.

The schematic of the heat exchange unit, and the layout of temperature and humidity probes based on the interference range in ref [27] were shown in Fig. 2a and b, respectively. Wherein T/W represented the temperature and humidity integrated probe, T represented the temperature probe.

The test soil sample was fine-grained sand with a particle size of 0.08 ~ 0.25mm, a dry density of 1570kg/m<sup>3</sup>, and a saturated moisture content of 23.7 %. The length, external diameter, and wall thickness of the heat exchange tube made of copper was 1200mm, 5mm, and 0.5mm, respectively. The fabricant and model, measurement range and accuracy of the other devices were shown in Table 1. The temperature and humidity were transmitted to the data logger by KEITHLEY 2701 and NHJLY2801, respectively.

In addition, the 24-hour heat preservation performance test had been carried out to verify the heat preservation performance of the heat exchange unit. Figure 3 shows the 24-hour temperature variation in the soil at position 1–6, 2–6, 3–6 and the ambient air temperature. It can be seen that the soil temperature at position 1–6, 2–6 and 3–6 is almost equal to each other, which almost does not change with heat transfer time, indicating that the heat exchange unit meets the requirement of insulation performance.

The uncertainty analysis was carried out using the secondary power method presented in ref [28], that is parameter  $Y = f(X_1, X_2, X_n)$ , wherein  $X_1, X_2, X_n$  are independent variables, and their uncertainties follow normal distribution, and then,

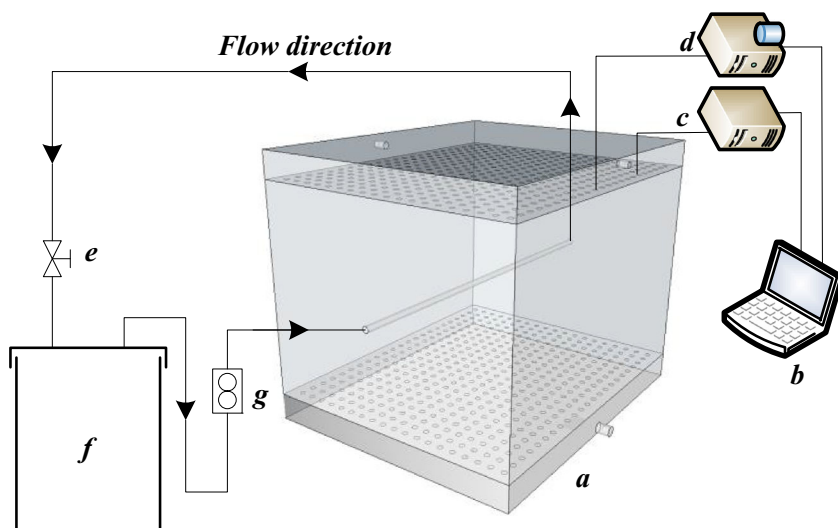
$$\Delta Y = \sqrt{\sum_{i=1}^n \left( \frac{\partial Y}{\partial X_i} \Delta X_i \right)^2} \quad (1)$$

The relative uncertainty of parameter Y can be expressed as:

$$\frac{\Delta Y}{Y} = \sqrt{\sum_{i=1}^n \left( \frac{\Delta X_i}{X_i} \right)^2} \quad (2)$$

In this study, the temperature of circulating fluid is within the range of 6 ~ 46 , and the maximum variation of soil temperature is within the range 17 ~ 34 . So, the maximum uncertainty of the temperature measured by the devices in Table 1 is:

**Fig. 1** Schematic of experimental setup for heat storage and release in soils. **a** Heat exchange unit **b** Data Logger **c** Humidity acquisition unit **d** Temperature acquisition unit **e** Throttle **f** Thermostatic water bath **g** Glass rotor flowmeter



$$\frac{\Delta T}{T} = \sqrt{\left(\frac{0.1}{6}\right)^2 + \left(\frac{0.24}{6}\right)^2 + \left(\frac{0.1}{17}\right)^2} = 4.4\% \quad (3)$$

For the glass rotor flowmeter in Table 1, the maximum uncertainty of mass flow is 5.8 %, under the setting experimental condition(170L/h).

### 3 Methods and results

In order to analyze the soil temperature distribution in the process of heat storage and release, and observe the influence rules of moisture content and heat source temperature on that.

The temperature distribution of the soil with different moisture content were experimentally studied, under different excess temperature.

The excess temperature  $\theta$  ( ) was defined by Eq. (4).

$$\theta = T_f - T_s \quad (4)$$

Where  $T_f$  ( ) is the inlet temperature of the fluid in tube,  $T_s$  ( ) is the initial soil temperature. When the value of  $\theta$  is positive, the inlet temperature is higher than the initial soil temperature, that is soil heat storage process. When the value of  $\theta$  is negative, the inlet temperature is lower than the initial soil temperature, that is soil heat release process.

The excess temperature difference  $\Delta\theta$  ( ) was defined by Eq. (5).

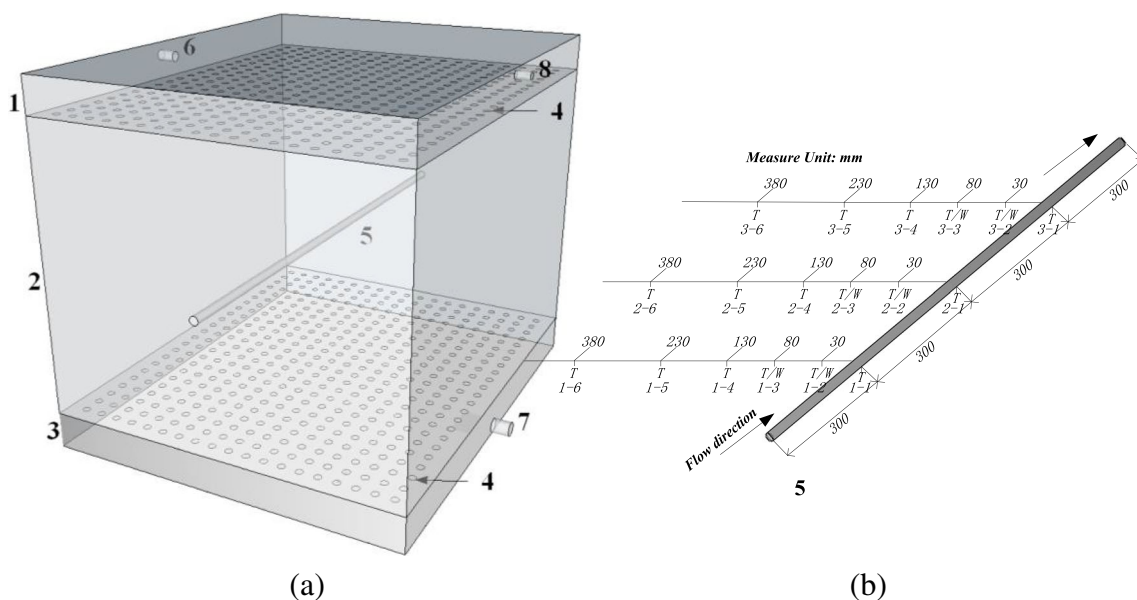


**Fig. 2** The structure of the heat exchange unit. **a** Schematic of heat exchange unit **b** Layout of temperature and humidity probes. (1) Feed-water Tank (2) Heat Exchange Sandbox (3) Drainage Bunker (4) Pervious Layer (5) Heat Exchange Tube (6) Water injection (7) Water drainage (8) Overfall Gap

**Table 1** The experimental instrumentation

Device	Fabricant and Model	Measurement Accuracy	Measurement (Adjustment) Range
Temperature and humidity integrated probe	Zhongke Nenghui in Wuhan NHSF48	$\pm 0.1^{\circ}\text{C}$ $\pm 1.0\%$	$-40^{\circ}\text{C} \sim +80^{\circ}\text{C}$ $0\% \sim 100\%$
Temperature probe	Weilian in Shanghai Pt100	$\pm(0.15+2.0 \times 10^{-3} \times t)$	$-200 \sim +850$
Thermostatic water bath	Tianheng in Ningbo THD-3006H	$\pm 0.1$	$-30 \sim +100$
Glass rotor flowmeter	Xiangjin in Taizhou LZB-15	2.5%	40L/h~400L/h

$$\Delta\theta = T - T_s \quad (5)$$

Where  $T$  ( ) represented the soil temperature at a certain measuring point during the heat transfer process. During heat storage process, the excess temperature difference  $\Delta\theta$  was expressed as  $\Delta\theta_S$ , and during heat release process, the excess temperature difference  $\Delta\theta$  was expressed as  $\Delta\theta_R$ .

The soil temperature change deviation  $\varepsilon$  was defined by Eq. (6).

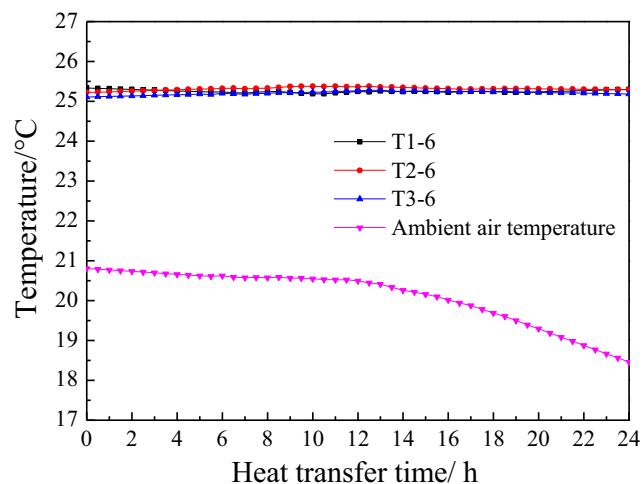
$$\varepsilon = \frac{|\Delta\theta_S| - |\Delta\theta_R|}{|\Delta\theta_S|} \quad (6)$$

The soil moisture content  $\omega$  (%) was defined by Eq. (7).

$$\omega = \frac{M_h - M_d}{M_d} \times 100 \quad (7)$$

Where  $M_h$  (kg) and  $M_d$  (kg) respectively represented the quality of wet and dry soils.

In order to ensure turbulent state, the flow rate in tube was set to be constant at 170L/h (0.7m/s) during experimental.

**Fig. 3** Soil temperature variation in heat preservation test

### 3.1 Excess temperature difference distributions of the soil in drying state

Under the environment condition, the minimum soil moisture content is 2.3 %. So, the soil moisture content 2.3 % was considered as drying state. At  $\theta = \pm 15$ , the heat storage and release experiments in the soil (initial soil temperature of  $26^{\circ}\text{C}$ ) under drying state was conducted for 6 hours, respectively. The excess temperature difference ( $\Delta$ ) distributions with time at position 2–2 are shown in Fig. 4a, and the radial excess temperature difference ( $\Delta$ ) distributions after the soil heat storage and release processes, at 600mm away from the water inlet, are shown in Fig. 4b.

As can be seen from Fig. 4a, the excess temperature difference distributions with time at position 2–2 during soil heat storage and release processes are almost symmetric. The excess temperature difference increases (decreases) gradually with time during heat storage (release) process. As the heat transfer process progresses, the change rate of excess temperature difference decreases, due to the temperature gradient between the fluid in tube and the surrounding soil gradually decreases. From Fig. 4b, it can be seen that, at 600mm away from the fluid inlet, the radial excess temperature difference distributions of the soil are also almost symmetric. The differences in excess temperature difference at position 2–2, 2–3, 2–4, 2–5 was 3.0 %, 4.3 %, 3.8 %, and 4.1 % respectively. The excess temperature difference decreases as the distance from the tube wall increases, due to the soil around tube is the main heat transfer resistance, which has attenuation effect on the heat transfer. Therefore, it could be concluded that, under the same excess temperature, the temperature distributions of the test soil sample in drying state during heat storage and release processes are almost symmetric, indicating the randomness of the pores distribution of the fine-grained sand in drying state has almost negligible influence on heat transfer, for the selected fine-grained sand particles are relatively uniform and stable in physical properties.

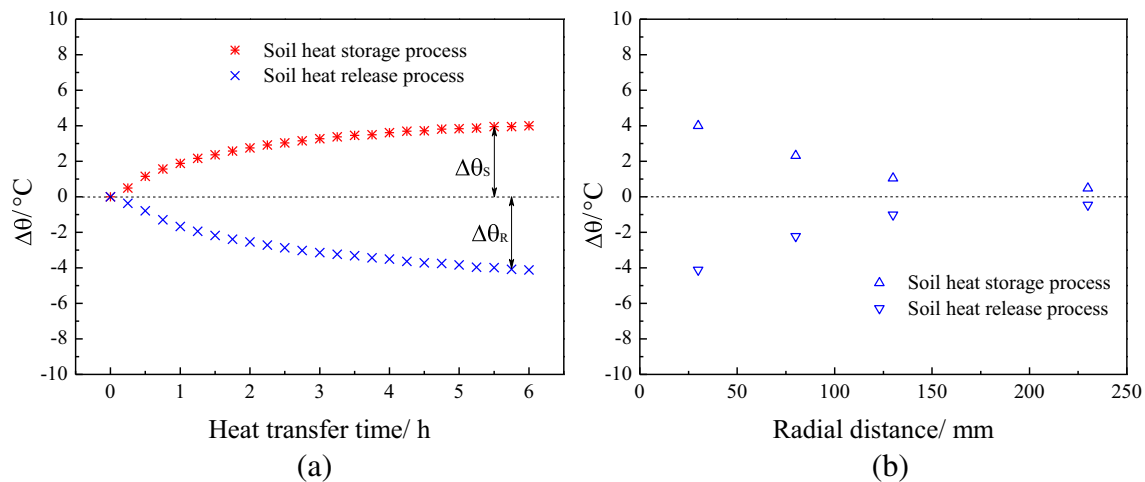


**Fig. 4** Excess temperature difference ( $\Delta$ ) distributions in heat storage and release processes ( $\theta = \pm 15^\circ\text{C}$ ,  $\omega = 2.3\%$ ). (a) position 2–2 (b) 600mm away from the water inlet,  $\tau = 6$  h

### 3.2 Excess temperature difference distributions of the soil in unsaturated and saturated state

Considering that the soil around ground heat exchanger is almost unsaturated or saturated, therefore, the heat storage and release experiments of unsaturated and saturated soil would be carried out. The test soil sample had a moisture content of 2.3% in drying state and 23.7% in saturated state. The intermediate values of 10.2%, 15.7% and 20.5% were taken as the unsaturated soil moisture content.

#### 3.2.1 Excess temperature difference distributions with time

At each set of excess temperature ( $\theta = \pm 5^\circ\text{C}$ ,  $\pm 10^\circ\text{C}$ ,  $\pm 15^\circ\text{C}$ ,  $\pm 20^\circ\text{C}$ ), the heat storage and release experiments of the soil (initial soil temperature of  $26^\circ\text{C}$ ) with moisture content of 10.2% was conducted for 6 hours, respectively, the excess temperature difference ( $\Delta$ ) distributions with time at position 2–2 are shown in Fig. 5a. The heat storage and release experiments of the soil with the other moisture content (15.7%, 20.5%, and 23.7%) at each set of excess temperature ( $\theta$ ) would also be carried out for 6 hours, respectively, the excess temperature difference ( $\Delta$ ) distributions with time at position 2–2 are shown in Fig. 5b-d.

It can be seen from Fig. 5a that, during heat storage and release processes under each set of excess temperature, the excess temperature difference distributions with time of the soil with moisture content of 10.2% are almost symmetric, and the soil temperature change rate increases as the excess temperature increases, for the temperature difference driving potential increases. As can be seen from Fig. 5b-d, under each set of excess temperature, the distribution rules with time of excess temperature difference in the soil with the other moisture content are consistent with that in the soil with moisture content of

10.2%. It can be obtained from the experimental results, during heat storage and release processes under the same excess temperature, the excess temperature difference distributions with time of the test soil sample in unsaturated or saturated state is almost symmetric, indicating although the saturated or unsaturated fine-grained sand has different forms of heat and mass transfer (solid heat conduction and phase change heat transfer, liquid water migration and vapor water diffusion) due to the random distribution of pores during heat storage and release processes, the influence of that on the temperature distribution of fine-grained sand, a relatively homogeneous porous medium, during the process of heat storage and release can be almost ignored.

The results of the excess temperature difference ( $\Delta$ ) distributions with time at position 2–2 in the soil with different moisture content ( $\omega$ ) and excess temperature ( $\theta$ ) are shown in Fig. 6a-d, respectively.

It can be observed from Fig. 6a-d that, the excess temperature difference distributions with time almost does not change with the moisture content under each set of excess temperature. Indicating that, for the fine-grained sand, the influence of the change of moisture content on the heat transfer performance of that is almost negligible. There are also experimental studies [29, 30] have shown that, as the moisture content of fine-grained sand increases from drying state to saturated state, the air in the pores is gradually replaced by liquid water, and the overall thermal conductivity increases obviously for the thermal conductivity of liquid water is about 20 times that of air. After reaching a certain level, most of air is replaced by liquid water, and the thermal conductivity of fine-grained sand almost no longer increases with the increase of moisture content. From observing Figs. 4a and 6c, it can be proved that the above experimental results are reasonable.

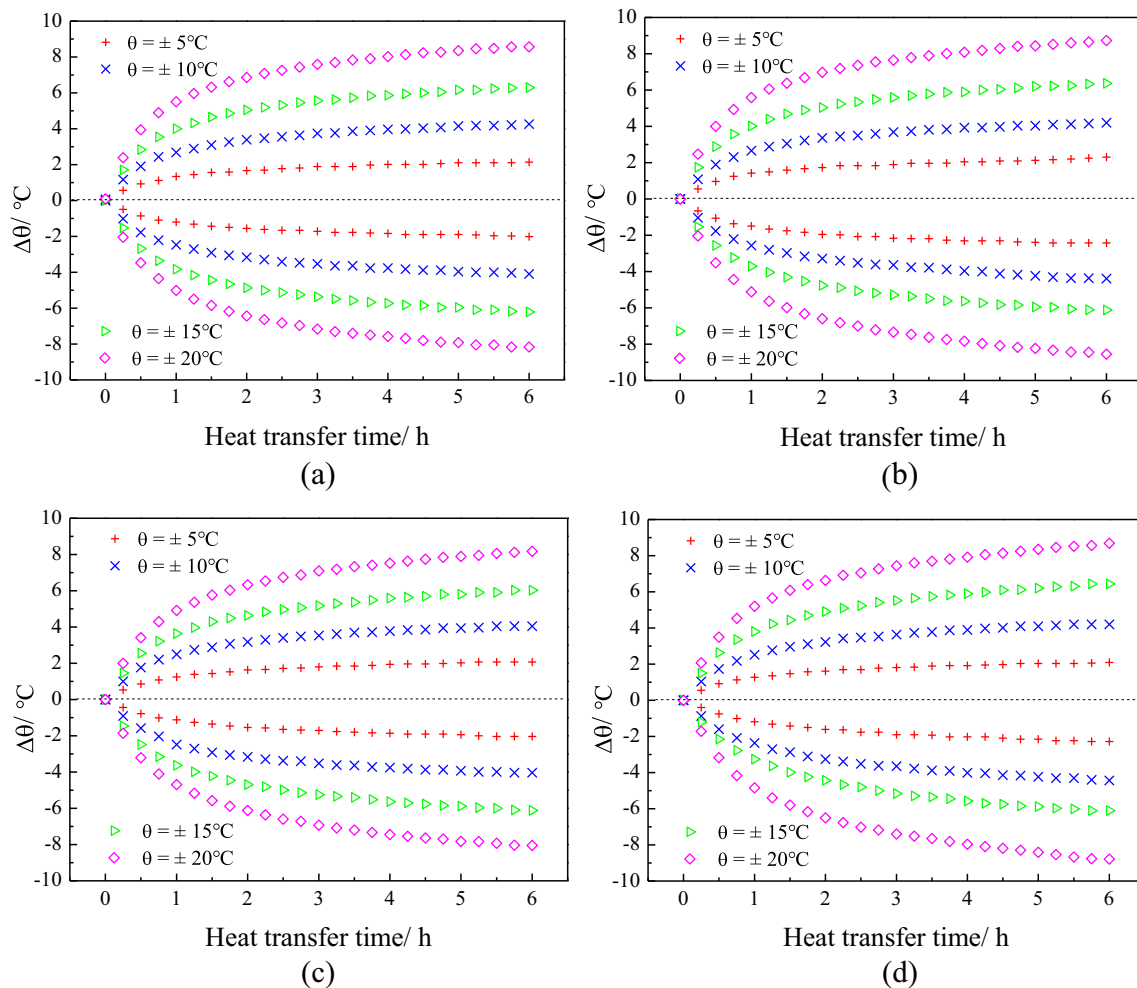


**Fig. 5** Excess temperature difference ( $\Delta$ ) variations vs. time at position 2–2 in the soil during heat storage and release processes under each set of excess temperature ( $\theta$ ). (a)  $\omega = 10.2\%$  (b)  $\omega = 15.7\%$  (c)  $\omega = 20.5\%$  (d)  $\omega = 23.7\%$

Since the influence of moisture content on the excess temperature difference distribution with time is almost negligible. Therefore, the excess temperature difference change trend versus time in the soil with moisture content of 15.7% during heat storage and release processes under each set of excess temperature was performed for fitting analysis. Results are shown in Table 2.

It can be perceived from Table 2 that, there is a good logarithmic relationship between the soil temperature change and the heat transfer time under each set of excess temperature, and the greater the excess temperature, the faster the soil temperature changes with time during heat storage and release processes. According to Table 2, the maximum temperature change deviation is  $-5.2\%$ .

### 3.2.2 Excess temperature difference distributions in radial direction

In order to observe the characteristics of radial temperature distribution in the soil after heat storage and release

processes, under each set of excess temperature ( $\theta$ ), the results of the excess temperature difference ( $\Delta$ ) distributions along radial distance in the soil with moisture content ( $\omega$ ) of 10.2%, 15.7%, 20.5%, and 23.7%, at 600mm away from the water inlet, are shown in Fig. 7a–d, respectively.

From Fig. 7a–d, it can be seen that the radial excess temperature difference distributions are all almost symmetric. The excess temperature difference increases with the increase of excess temperature, and decreases with the increase of the distance away from the tube wall, and the closer to the tube wall, the greater the variation with excess temperature of excess temperature difference, indicating the stronger the temperature disturbance.

The results of the radial excess temperature difference ( $\Delta$ ) distributions under different excess temperature ( $\theta$ ) at 600mm away from the water inlet in the soil with different moisture content ( $\omega$ ) are shown in Fig. 8a–d, respectively.

It can also be observed from Fig. 8a–d that, the excess temperature difference distributions along radial distance

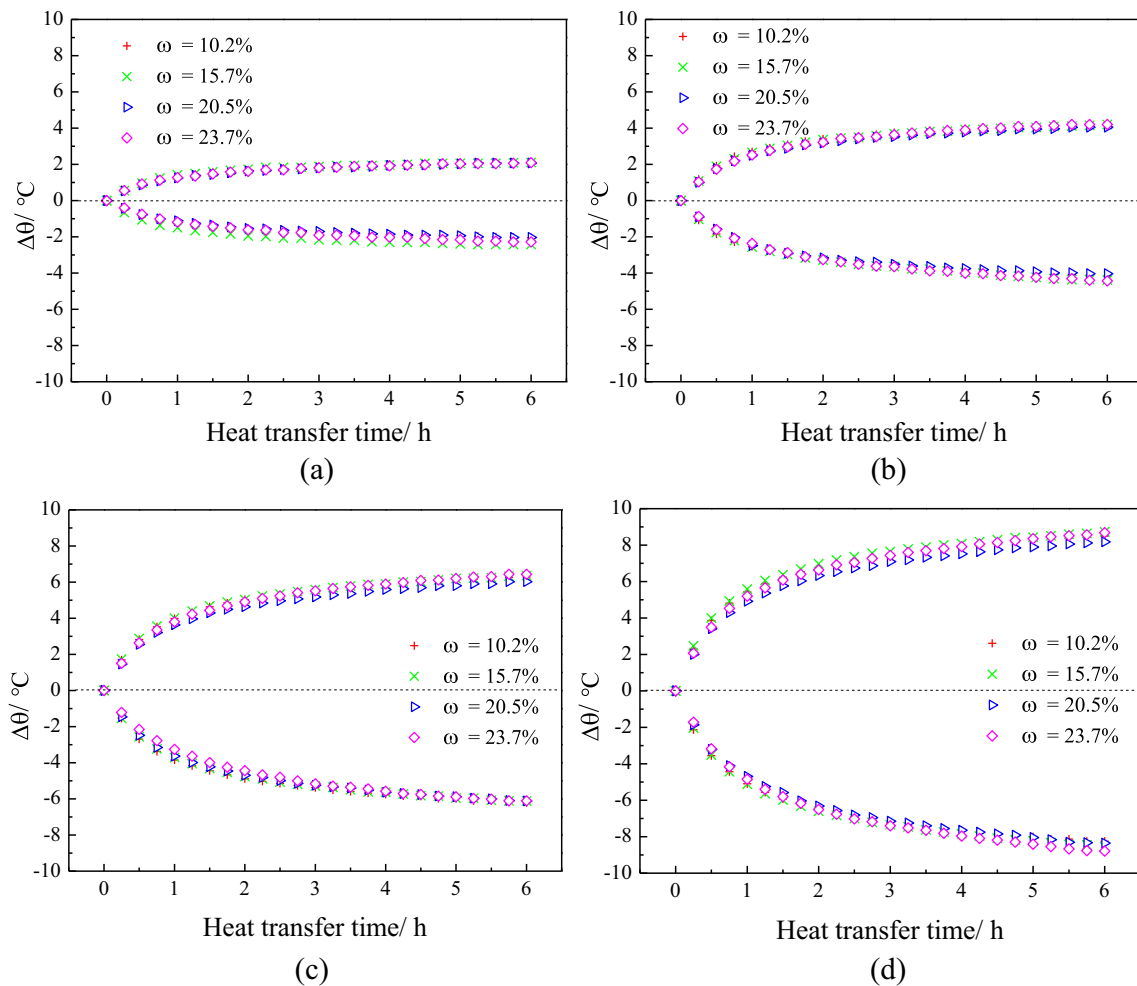


**Fig. 6** Excess temperature difference ( $\Delta$ ) variations vs. time at position 2–2 in the soil with different moisture content ( $\omega$ ) during heat storage and release processes. (a) =  $\pm 5$  (b) =  $\pm 10$  (c) =  $\pm 15$  (d) =  $\pm 20$

almost does not change with the moisture content under each set of excess temperature. That is, within the range of moisture content of 10.2 %–23.7 %, the change of moisture content has almost no effect on the radial excess temperature difference distribution of the soil under each set of excess temperature.

The radial excess temperature difference distribution of the soil with moisture content of 15.7 % under each set of excess

temperature was performed for fitting analysis, results are shown in Table 3.

It can be obtained from Table 3 that, the soil temperature change amount after heat storage and release processes under each set of excess temperature is also in a good logarithmic relationship with the radial distance, and the greater the excess temperature, the faster the soil temperature changes with radial distance after heat storage and release processes. According to Table 3, the maximum temperature change deviation is - 5.3 %.

In the study of Hedayati-Dezfooli et al. [19], under the condition of the top and bottom boundaries are constant at + 90 and + 10 , the one-dimension vertical heat and moisture transfer in silt clay/sand (29 %/71 %) with moisture content of 26 % was experimentally studied. It can be obtained from that, after the 2.5 h heat transfer process, the central position temperature at 15mm, 45mm, and 75mm away from the top boundary is 75.6 , 63.1 , and 55.1 , respectively. Indicating the longitudinal soil temperature also shows a good logarithmic distribution by fitting analysis.

**Table 2** The fitting relationship between  $\Delta_S$ ,  $\Delta_R$  and the heat transfer time ( $\tau$ ), and the  $\varepsilon$  under each set of  $\Delta$  (at position 2–2,  $\omega = 15.7\%$ )

( $\Delta$ )	$\Delta_S$ (°C)	$\Delta_R$ (°C)	$\varepsilon$ ( $\tau=6$ h)
$\pm 5$	$\Delta_S = 0.47\ln(\tau)+1.42$ $R^2 = 0.9872$	$\Delta_R = - 0.52\ln(\tau) - 1.45$ $R^2 = 0.9926$	-5.2%
$\pm 10$	$\Delta_S = 0.9\ln(\tau)+2.64$ $R^2 = 0.9867$	$\Delta_R = - 1.09\ln(\tau) - 2.49$ $R^2 = 0.9986$	-4.4%
$\pm 15$	$\Delta_S = 1.38\ln(\tau)+3.94$ $R^2 = 0.9901$	$\Delta_R = - 1.48\ln(\tau) - 3.67$ $R^2 = 0.9971$	1.4%
$\pm 20$	$\Delta_S = 1.87\ln(\tau)+5.45$ $R^2 = 0.991$	$\Delta_R = - 2.07\ln(\tau) - 5.03$ $R^2 = 0.9968$	0.7%

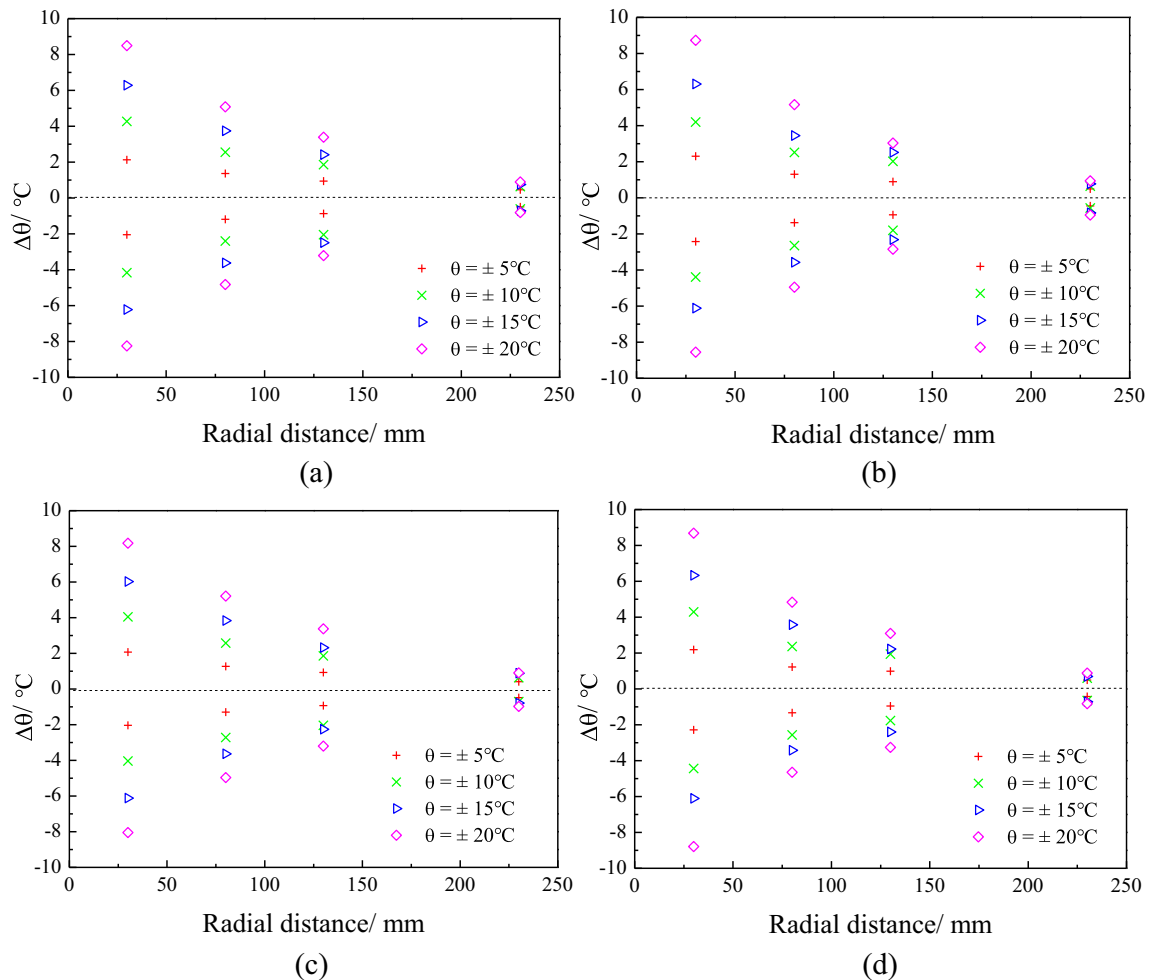


**Fig. 7** Excess temperature difference ( $\Delta$ ) distributions along radial distance of the soil at 600mm away from the water inlet under each set of excess temperature ( $\theta$ ). ( $\tau = 6$  h). (a)  $\omega = 10.2\%$  (b)  $\omega = 15.7\%$  (c)  $\omega = 20.5\%$  (d)  $\omega = 23.7\%$

### 3.2.3 Excess temperature difference distributions in longitudinal direction

In order to observe the distribution characteristics of the soil temperature along the longitudinal distance after heat storage and release processes, under each set of excess temperature ( $\theta$ ), the results of the excess temperature difference ( $\Delta$ ) distributions along longitudinal distance in the soil with moisture content ( $\omega$ ) of 10.2%, 15.7%, 20.5%, and 23.7%, at 30mm away from the tube wall, are shown in Fig. 9a-d, respectively.

It can be perceived from Fig. 9a-d that the longitudinal excess temperature difference distributions are also almost symmetrical. As the heat transfer process proceeds along the tube, the farther away from the water inlet, the smaller the temperature gradient between the fluid in the tube and the surrounding soil, and the smaller the excess temperature difference changes with excess temperature.

The results of the longitudinal excess temperature difference ( $\Delta$ ) distributions under different excess

temperature ( $\theta$ ) at 30mm away from the tube wall in the soil with different moisture content ( $\omega$ ) are shown in Fig. 10a-d, respectively.

It can be obtained from Fig. 10a-d that, under each set of excess temperature, there are almost no differences in the longitudinal excess temperature difference distributions of the soil with different moisture content. It shows that within the range of moisture content of 10.2%-23.7%, the influence of the change of moisture content on the longitudinal excess temperature difference distribution of the soil can be ignored.

The longitudinal excess temperature difference distribution of the soil with moisture content of 15.7% under each set of excess temperature was performed for fitting analysis, results are shown in Table 4.

It can be obtained from Table 4 that, the soil temperature change amount after heat storage and release processes under each set of excess temperature is also in a good logarithmic relationship with the longitudinal distance, and the greater the excess temperature, the faster the soil temperature changes with longitudinal distance after heat storage and release



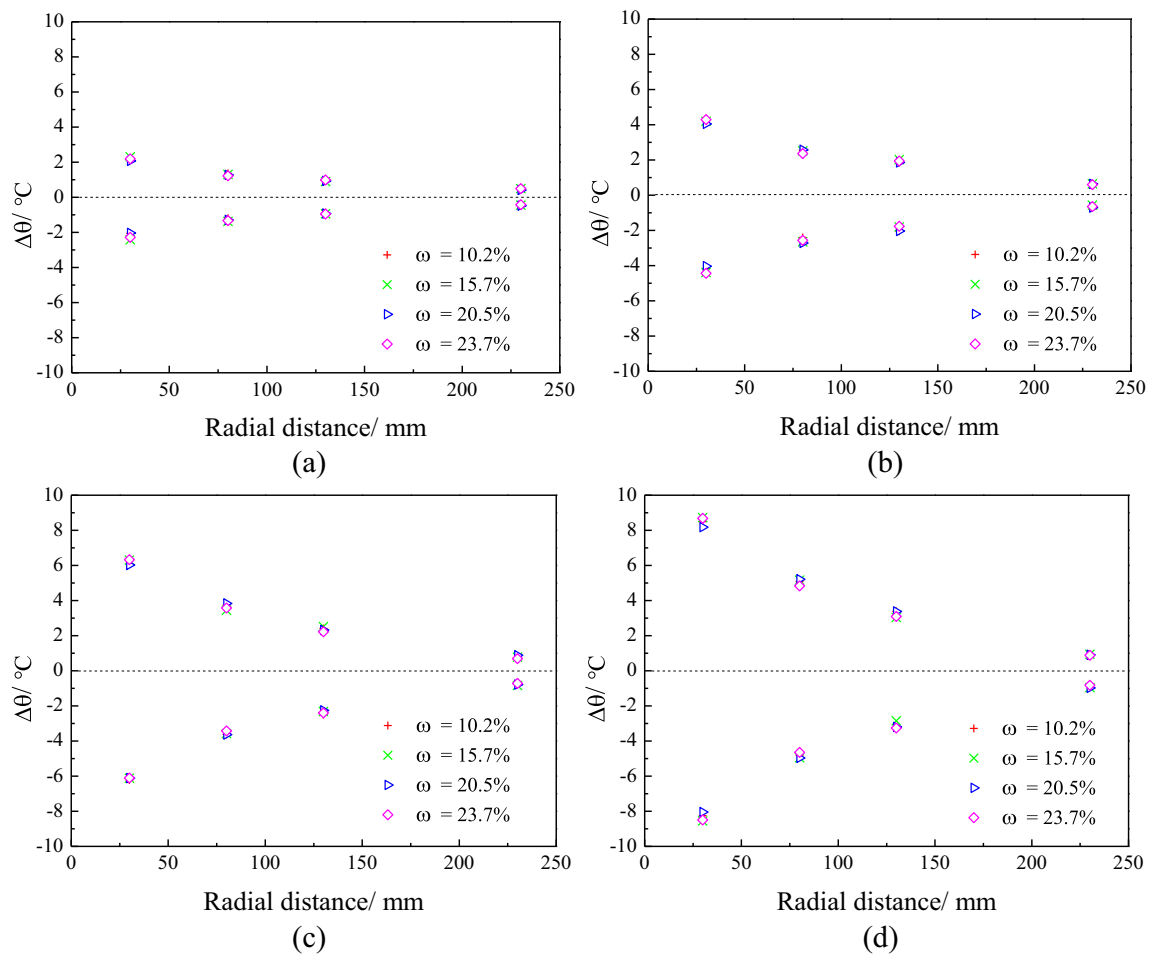


**Fig. 8** Excess temperature difference ( $\Delta$ ) distributions along radial distance of the soil with different moisture content ( $\omega$ ) at 600mm away from the water inlet. ( $\tau=6$  h). (a)  $\pm 5$  (b)  $\pm 10$  (c)  $\pm 15$  (d)  $\pm 20$

processes. According to Table 4, the maximum temperature change deviation is 2.5 %.

### 3.3 Excess temperature difference change with the excess temperature

From the above analysis, during soil heat storage and release processes, the soil temperature distributions with time and space are almost symmetric, and the influence of the change

of moisture content on the soil temperature distribution can be almost negligible. Therefore, the relationship between the soil temperature change during heat storage process ( $\Delta_s$ ) and the excess temperature ( $\Delta$ ) in the soil with moisture content of 15.7 % was analyzed. The results of the change trend of  $\Delta_s$  versus  $\Delta$  in the soil at different distances away from the tube wall and the water inlet are shown in Fig. 11a-b.

It can be perceived from Fig. 11a-b that the  $\Delta_s$  at radial and longitudinal directions all show a linear

**Table 3** The fitting relationship between  $\Delta_s$ ,  $\Delta_R$  and the radial distance away from the tube wall ( $r$ ), and the  $\varepsilon$  under each set of  $\Delta$  (at 600mm away from the water inlet,  $\omega = 15.7\%$ ,  $\tau = 6$  h)

$\Delta$	$\Delta_s$ ( $r$ )	$\Delta_R$ ( $r$ )	$\varepsilon$ ( $r=30\text{mm}$ )
$\pm 5$	$\Delta_s = -0.9\ln(r) + 5.33$ $R^2 = 0.9926$	$\Delta_R = 0.97\ln(r) - 5.69$ $R^2 = 0.9973$	-5.3%
$\pm 10$	$\Delta_s = -1.69\ln(r) + 9.98$ $R^2 = 0.9847$	$\Delta_R = 1.86\ln(r) - 10.75$ $R^2 = 0.9976$	-4.5%
$\pm 15$	$\Delta_s = -2.68\ln(r) + 15.36$ $R^2 = 0.9956$	$\Delta_R = 2.59\ln(r) - 14.94$ $R^2 = 1$	1.8%
$\pm 20$	$\Delta_s = -3.85\ln(r) + 21.87$ $R^2 = 0.9989$	$\Delta_R = 3.77\ln(r) - 21.37$ $R^2 = 0.9985$	2.5%

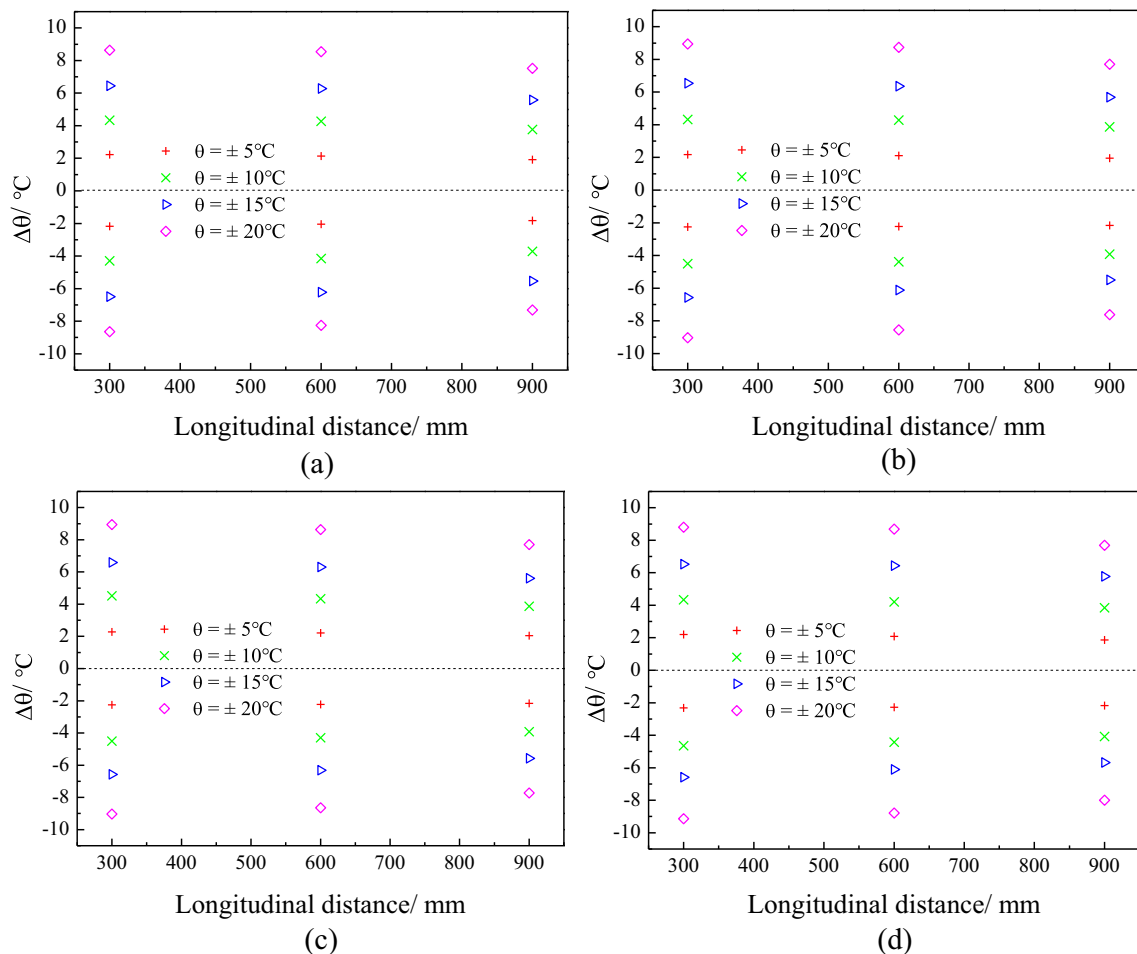


**Fig. 9** Excess temperature difference ( $\Delta$ ) distributions along longitudinal distance of the soil at 30mm away from the tube wall under each set of excess temperature ( $\theta$ ). ( $\tau = 6$  h). (a)  $\omega = 10.2\%$  (b)  $\omega = 15.7\%$  (c)  $\omega = 20.5\%$  (d)  $\omega = 23.7\%$

increase trend with  $\Delta$ , indicating that relative to the moisture migration during heat transfer process, the excess temperature is the main factor affecting the soil temperature change. It also can be seen from Fig. 11a-b that the change rate of  $\Delta_S$  with  $\Delta$  decreases as the radial or longitudinal distance increases, it is proved that the closer to the tube wall or the water inlet, the stronger the soil temperature disturbance. From comparing Fig. 11a and b, it can be obviously observed that the slope between  $\Delta$  and  $\Delta_S$  changes with radial distance is much greater than that with longitudinal distance, thus it can be obtained that the soil temperature disturbance in radial direction is far greater than that in longitudinal direction.

In the study of Gao et al. [31], the one-dimension horizontal heat and moisture transfer in silt clay/sand (28.7%/71.3%) with moisture content of 9.2% was experimentally studied. It can be concluded from that, after the 6 h heat transfer under the temperature difference of +18, +28, and +37, at a distance of 30mm away from the heat source, the soil temperature increased by 15, 22.8, and 31.5, respectively. Indicating that there is also a linear relationship between soil temperature

change and heat transfer temperature difference, by fitting analysis.

#### 4 Regression analysis of experimental data

The excess temperature difference ( $\Delta$ ) of the soil with moisture content of 15.7% during heat storage process is subjected to regression analysis. Since there are four main factors affecting the temperature distribution of the test soil sample, which is excess temperature ( $\theta$ , within the range of  $\pm 5 \sim \pm 20$ ), radial distance ( $r$ , within the range of 30mm~230mm), longitudinal distance ( $l$ , within the range of 300mm~900mm), and heat transfer time ( $\tau$ , within the range of 0~6hours). Thus, there are four independent variables and one dependent variable in the regression analysis. The relationship between the independent variables and the dependent variable is nonlinear, it belongs to the multivariate nonlinear regression analysis.

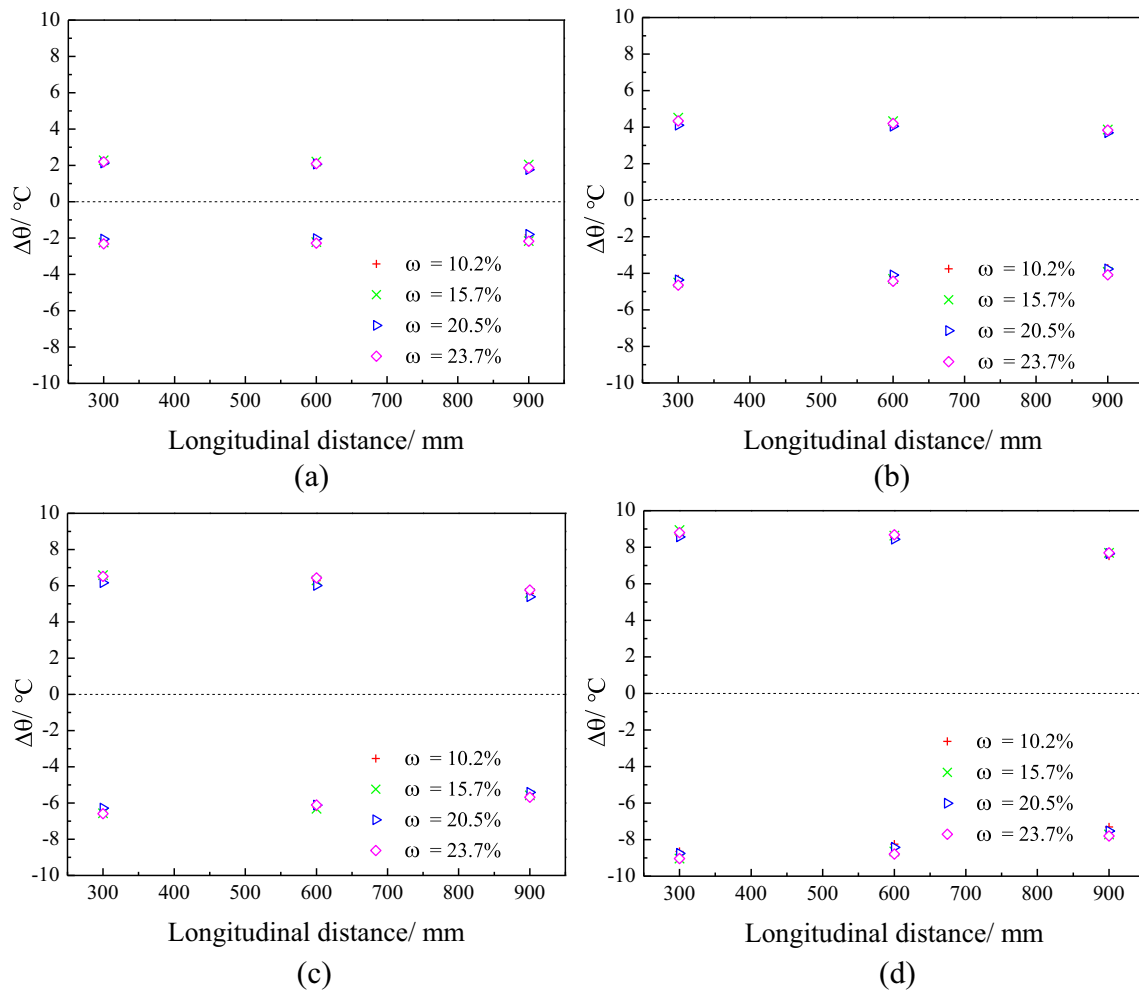


**Fig. 10** Excess temperature difference ( $\Delta$ ) distributions along longitudinal distance of the soil with different moisture content ( $\omega$ ) at 30mm away from the tube wall. ( $\tau = 6$  h). (a)  $\pm 5$  (b)  $\pm 10$  (c)  $\pm 15$  (d)  $\pm 20$

First assume that the regression model is a power function model, as defined by Eq. (8).

$$\Delta\theta = a \cdot \theta^b \cdot r^c \cdot \tau^d \cdot l^e \tag{8}$$

Then convert the power function model to linear form, as defined by Eq. (9).

$$\ln \Delta\theta = \ln a + b \ln \theta + c \ln r + d \ln \tau + e \ln l \tag{9}$$

So, the processed experimental data can be performed for linear regression analysis by the software SPSS, results are shown in Table 5.

It can be seen from Table 5 that the probability of the model is false is  $5.83E-79$ , and the R Square is 0.963, indicating that

**Table 4** The fitting relationship between  $\Delta_S$ ,  $\Delta_R$  and the longitudinal distance away from the water inlet ( $l$ ), and the  $\varepsilon$  under each set of  $\varepsilon$  (at 30mm away from the tube wall,  $\omega = 15.7\%$ ,  $\tau = 6$  h)

( $\varepsilon$ )	$\Delta_S$ ( $^{\circ}$ )	$\Delta_R$ ( $^{\circ}$ )	$\varepsilon$ ( $l=600\text{mm}$ )
$\pm 5$	$\Delta_S = -0.09\ln(l) + 2.82$ $R^2 = 0.9984$	$\Delta_R = 0.08\ln(l) - 2.7$ $R^2 = 0.9948$	2.5%
$\pm 10$	$\Delta_S = -0.55\ln(l) + 7.75$ $R^2 = 0.9993$	$\Delta_R = 0.5\ln(l) - 7.4$ $R^2 = 0.9927$	0.7%
$\pm 15$	$\Delta_S = -0.85\ln(l) + 11.51$ $R^2 = 0.9836$	$\Delta_R = 0.84\ln(l) - 11.47$ $R^2 = 0.9929$	0.4%
$\pm 20$	$\Delta_S = -1.06\ln(l) + 15.07$ $R^2 = 0.9923$	$\Delta_R = 1.12\ln(l) - 15.54$ $R^2 = 0.9829$	1.0%

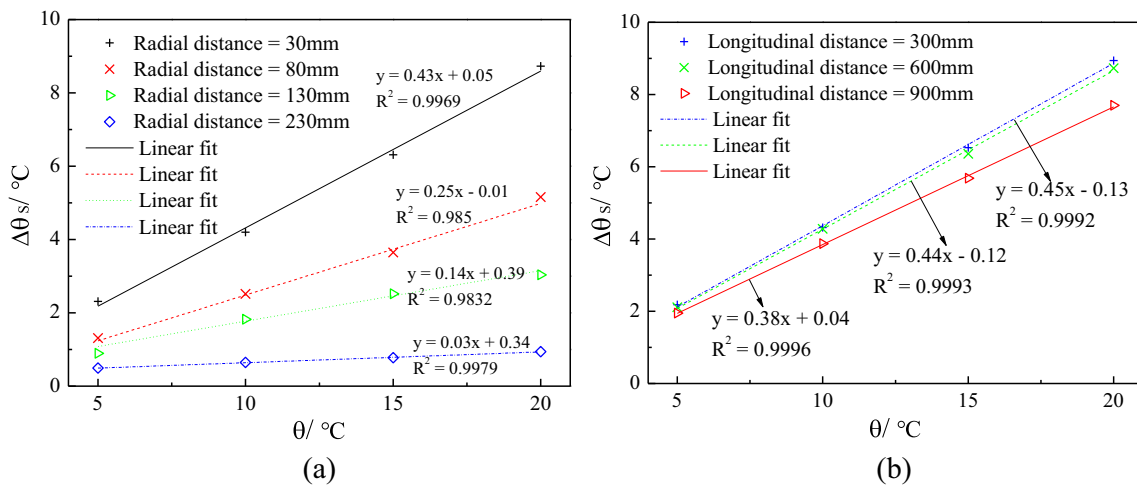


Fig. 11 The relationship between  $\Delta \theta_s$  and  $\theta$  in the soil with  $\omega = 15.7\%$ . ( $\tau = 6$  h). (a)  $l = 600$ mm (b)  $r = 30$ mm

the fitting degree between the estimated values and the actual values is high. After conducting the antilog, the empirical correlation between soil temperature change and various influencing factors can be obtained as Eq. (10), under the setting experimental conditions.

$$\Delta \theta = 7.925 \cdot \theta^{0.952} \cdot \tau^{0.332} \cdot r^{(-0.838)} \cdot l^{(-0.075)} \quad (10)$$

In order to verify the prediction deviation of Eq. (10), during the heat transfer process at  $\theta = +5, +10, +15,$  and  $+20$ , the predicted and actual  $\Delta \theta$  of the soil at position 2–2 with moisture content of 15.7% were taken for deviation analysis, results are shown in Fig. 12.

It can be observed from Fig. 12 that, the predicted values are close to the actual values, and the overall prediction deviation of Eq. (10) is almost within 10%.

### 5 Conclusions

The following conclusions can be obtained through the heat storage and release experiments in the fine-grained sand with different moisture content.

Table 5 Regression analysis results

	Coefficients	P-value	Significance F	R Square
Intercept	2.071	0.268	5.83E-79	0.963
X Variable 1	0.952	9.43E-70		
X Variable 2	-0.838	3.37E-58		
X Variable 3	-0.075	4.33E-42		
X Variable 4	0.332	0.04		

Under the same excess temperature, the temperature distribution in the process of soil heat storage and release is almost symmetric. The influence of the change of moisture content on the heat transfer performance of the wet test soil sample is almost negligible. The excess temperature is the main factor affecting the soil temperature change.

The soil temperature change in heat storage and release processes at each set of excess temperature are all in a good logarithmic relationship with the heat transfer time, radial distance and longitudinal distance. The correlation between soil temperature change and heat transfer time, radial distance, longitudinal distance is increase with the increase of excess temperature. The soil temperature change showed a linear increase trend with excess temperature, and the soil temperature disturbance in radial direction is far greater than that in longitudinal direction.

During heat storage and release processes under the setting experimental conditions, the experience formula has been obtained to predict the temperature change of the fine-grained

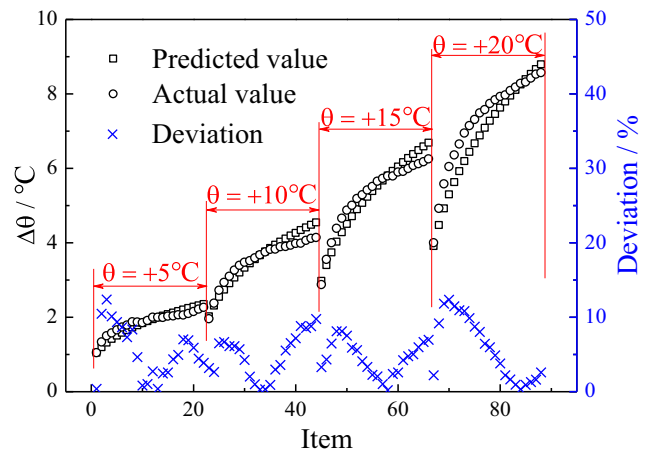


Fig. 12 Deviation analysis for the predicted and actual values

sand. The moisture migration characteristics in the fine-grained sand and the couple heat and moisture migration in the other soils would be reported in future.

## Declarations

**Conflict of interest** We declare that we do not have any commercial or associative interest that represents a conflict of interest in connection with the work submitted.

## References

- Philip JR, De Vries DA (1957) Moisture movement in porous materials under temperature gradient[J]. *EOS Trans Am Geophys Union* 38(2):222–232
- Luikov AV (1964) Heat and mass transfer in capillary-porous bodies[J]. *Adv Heat Tran* 1(1):123–184
- Chen Y, Shi M, Li X (2006) Experimental investigation on heat, moisture and salt transfer in soil [J]. *Int Commun Heat Mass Transfer* 33(9):1122–1129
- Nield DA, Bejan A (1992) *Convection in porous media[M]. Fundamentals of the finite element method for heat and fluid flow.* Wiley-Blackwell, Hoboken
- Chen Y, Feng J, Shi M (1998) Mathematical model of coupled heat and mass transfer in unsaturated soils[J]. *Pedosphere* 8(2):105–112
- Kayaci N, Demir H (2018) Long time performance analysis of ground source heat pump for space heating and cooling applications based on thermo-economic optimization criterion[J]. *Energy Build* 163:121–139
- Thomas K (1994) Simulation of simultaneous heat, and moisture transfer in a porous media with heated boundaries[D]. Rochester Institute of Technology. Accessed from <https://scholarworks.rit.edu/theses/5784>
- Dempsey BJ (1978) A mathematical model for predicting coupled heat and water movement in unsaturated soil[J]. *Int J Numer Anal Meth Geomech* 2(1):19–34
- Mottaghy D, Dijkshoorn L (2012) Implementing an effective finite difference formulation for borehole heat exchangers into a heat and mass transport code[J]. *Renew Energy* 45:59–71
- Li X, Zhao J, Zhou Q (2005) Inner heat source model with heat and moisture transfer in soil around the underground heat exchanger[J]. *Appl Therm Eng* 25(10):1565–1577
- Campbell GS, Jungbauer JDJR, Bidlake WR, Hungerford RD (1994) Predicting the effect of temperature on soil thermal conductivity[J]. *Soil Sci* 158(5):307–313
- Tarnawski VR, Gori F, Wagner B, Buchan GD (2000) Modelling approaches to predicting thermal conductivity of soils at high temperatures[J]. *Int J Energy Res* 24(5):403–423
- Wang Z, Wang F, Ma Z, Wang X, Wu X (2016) Research of heat and moisture transfer influence on the characteristics of the ground heat pump exchangers in unsaturated soil[J]. *Energy Build* 130:140–149
- Cui W, Gawecka KA, Potts DM, Taborda DMG, Zdravković L (2016) Numerical analysis of coupled thermo-hydraulic problems in geotechnical engineering[J]. *Geomech Energy Environ* 6:22–34
- Lien HP, Wittmann FH (1998) Mass transfer in inhomogeneous porous media under thermal gradients[J]. *Nucl Eng Des* 179(2):179–189
- Wang H, Qi C (2011) A laboratory experimental study of high-temperature thermal storage in the unsaturated soil using a vertical borehole heat exchanger[J]. *Int J Low Carbon Technol* 6(3):187–192
- Wang H, Qi C, Wang E, Du H, Li H (2010) Experimental study of heat and moisture transfer process for high-temperature heat storage of soils[J]. *Acta Energiæ Solaris Sinica* 31(7):824–828
- Wang H, Qi C, Wang E, Du H, Huang B (2011) Peak phenomenon of temperature and humidity during high-temperature heat storage in soil[J]. *Acta Energiæ Solaris Sinica* 32(4):490–494
- Hedayati-Dezfooli M, Leong WH (2019) An experimental study of coupled heat and moisture transfer in soils at high temperature conditions for a medium coarse soil[J]. *Int J Heat Mass Transf* 137:372–389
- Wang Y, Jiang C, Liu Y, Wang D, Liu J (2018) The effect of heat and moisture coupling migration of ground structure without damp-proof course on the indoor floor surface temperature and humidity: Experimental study[J]. *Energy Build* 158:580–594
- Liu BC, Liu W, Peng SW (2005) Study of heat and moisture transfer in soil with a dry surface layer[J]. *Int J Heat Mass Transf* 48(21/22):4579–4589
- Moradi A, Smits KM, Massey J, Cihan A, McCartney J (2015) Impact of coupled heat transfer and water flow on soil borehole thermal energy storage (SBTES) systems: Experimental and modeling investigation[J]. *Geothermics* 57:56–72
- Li HF, Chen MQ, Fu BA, Liang B (2019) Evaluation on the thermal and moisture diffusion behavior of sand/bentonite[J]. *Appl Therm Eng* 151:55–65
- Zhao J, Wang H, Li X, Dai C (2008) Experimental investigation and theoretical model of heat transfer of saturated soil around coaxial ground coupled heat exchanger[J]. *Appl Therm Eng* 28(2–3):116–125
- Kroener E, Vallati A, Bittelli M (2014) Numerical simulation of coupled heat, liquid water and water vapor in soils for heat dissipation of underground electrical power cables[J]. *Appl Therm Eng* 70(1):510–523
- Qin M, Ait-Mokhtar A, Belarbi R (2010) Two-dimensional hygrothermal transfer in porous building materials[J]. *Appl Therm Eng* 30(16):2555–2562
- Hedayati-Dezfooli M, Leong WH (2017) Experimental evaluation of the measurement errors of soil water content due to interference of two adjacent TDR probes[J]. *Exp Heat Transf* 30(4–6):475–488
- Moffat RJ (1988) Describing the uncertainties in experimental results[J]. *Exp Thermal Fluid Sci* 1(1):3–17
- Hong-Wang HF, Hua J (2015) Experimental study of thermal conductivity of common engineering soil with different water content[J]. *Water Resour Power* 33(12):122–124
- Nikiforova T, Savitskiy M, Limam K et al (2013) Methods and results of experimental researches of thermal conductivity of soils[J]. *Energy Procedia* 42:775–783
- Gao Y, Dong S, Wang C, Chen Y, Hu W (2020) Effect of thermal intensity and initial moisture content on heat and moisture transfer in unsaturated soil[J]. *Sustain Cities Soc* 55:1–13

**Publisher's note** Springer Nature remains neutral with regard to jurisdictional claims in published maps and institutional affiliations.